Engineering Reports

WILEY

Engineering Reports Open Access

RESEARCH ARTICLE OPEN ACCESS

Modeling of Inscribed Dual Band Circular Fractal Antenna for Wi-Fi Application Using Descartes Circle Theorem

SatheeshKumar Palanisamy[1] | Anitha R. Vaddinuri[1] | Arfat Ahmad Khan[2] | Muhammad Faheem[3]

[1]Department of ECE, BMS Institute of Technology and Management, Bengaluru, India | [2]Department of Computer Science, College of Computing, Khon Kaen University, Khon Kaen, Thailand | [3]School of Technology and Innovations, University of Vaasa, Vaasa, Finland

Correspondence: Muhammad Faheem (muhammfa@uwasa.fi)

Received: 24 May 2024 | **Revised:** 26 August 2024 | **Accepted:** 21 September 2024

Keywords: antenna | circle (DC) theorem | Descartes | fractal | front-to-back ratio

ABSTRACT

This study focuses on the modeling of a dual-band circular fractal antenna designed for Wi-Fi applications by utilizing the Descartes Circle Theorem. The antenna's geometry is characterized by self-similar fractal patterns, enabling enhanced performance in dual frequency bands relevant to Wi-Fi communication. Current research is trending towards the development of antennas capable of operating across various Wi-Fi bands, and the emerging 6 GHz band. In this article, there is also a focus on achieving ultra-wideband functionality to cater to the requirements of future wireless technologies. Incorporation with Circuits and Systems: Ongoing efforts are directed at seamlessly integrating these antennas with RF circuits and communication systems to enhance their practical utility and applicability. The exploration of unconventional fractal shapes and the utilization of advanced optimization algorithms present promising avenues for enhancing antenna performance and achieving miniaturization. This research contributes to the advancement of compact and efficient antenna designs for wireless communication systems. Detailed considerations are given to the 2.4 and 5.55 GHz bands to ensure compatibility with standard Wi-Fi protocols. The designed circular fractal antenna is compared with the conventional circular patch antenna and the results were analyzed. At the resonating frequency of 2.4 and 5.55 GHz, circular patch antenna has a reflection coefficient (S_{11}) of −18.1 and −13.51, respectively with a peak gain of 3.6 dBi, whereas, the designed circular fractal antenna shows an improved reflection coefficient, S_{11} of −22.0 and −15.5 dB at the same resonating frequency with a peak gain of 11.7920 dBi. The radiation pattern shows that the antenna radiated in unidirectional pattern with the front-to-back ratio of 101.4 which is higher than circular patch antenna. The miniaturized antenna is fabricated through photo etching process, tested, and validated.

1 | Introduction

In recent years, the demand for high-performance wireless communication systems has driven significant advancements in antenna technology. Among these advancements, fractal antennas have emerged as a promising solution due to their unique properties, such as multiband behavior and compact size. This study focuses on the modeling of an inscribed dual band circular fractal antenna designed for Wi-Fi applications, leveraging the principles of the Descartes Circle Theorem to achieve optimal performance. Fractal antennas, characterized by their self-similar patterns, offer numerous advantages, including wide bandwidth, high gain, and efficient space utilization. These attributes make them ideal for modern wireless communication systems that require antennas capable of operating over multiple frequency bands while maintaining a compact form factor. The Descartes Circle Theorem, a fundamental principle in geometry, provides a mathematical framework for constructing fractal shapes with precise circular arrangements, which can be applied to antenna design to enhance performance characteristics. The integration of dual-band functionality in a single antenna is particularly beneficial for Wi-Fi applications, where efficient spectrum utilization and minimal interference are crucial. The IEEE 802.11 Wi-Fi standards operate primarily in the 2.4 and 5 GHz frequency bands, making dual-band antennas essential for achieving seamless connectivity and high data rates. By employing fractal geometry, specifically the inscribed circular fractal pattern, the proposed antenna aims to achieve enhanced bandwidth and gain, thereby meeting the stringent requirements of contemporary Wi-Fi systems. It is analyzed that the problem faced by the Apollonian circle is overcome by using DC theorem. Enhancing the antenna gain involves the creation of an L slot on the bottom ground plane. The use of Coplanar Waveguide (CPW) enhances compatibility with compact wireless communication devices. A microstrip antenna array is designed with an Electromagnetic Band Gap (EBG) structure to improve reflection coefficient (S_{11}), directivity, and gain at a frequency of 5.85 GHz. The antenna design incorporates circular fractal patterns, utilizing self-similarity to enhance performance characteristics. The chosen geometry facilitates dual-band functionality. Through a parametric analysis involving the manipulation of key parameters such as the number of iterations, scaling factor, and feed position, researchers fine-tune the antenna design to achieve the desired resonant frequencies and bandwidths. After optimization in simulation, the antenna prototypes are created on appropriate substrates, and their real-world performance is assessed using network analyzers and antenna chambers to corroborate the simulation outcomes.

In this study, we designed an inscribed dual band circular fractal antenna with operational frequencies centered at 2.4 and 5.55 GHz, corresponding to the primary Wi-Fi bands. The antenna's dimensions were optimized to achieve a compact size of 50 mm × 50 mm, making it suitable for integration into various wireless devices. The application of the Descartes Circle Theorem allowed for precise placement of circular elements within the fractal structure, resulting in improved impedance matching and radiation efficiency. Simulation results demonstrated that the proposed antenna achieved a −10 dB return loss bandwidth of 200 MHz (2.35–2.55 GHz) for the 2.4 GHz band and 500 MHz (5.6–6.1 GHz) for the 5.55 GHz band. Additionally, the antenna exhibited a peak gain of 11.792 and 9.4 dBi for the 2.4 and 5.55 GHz bands, respectively. These performance metrics indicate that the inscribed dual band circular fractal antenna can effectively meet the demands of high-speed Wi-Fi applications, providing reliable connectivity and enhanced coverage.

This paper explores the theoretical foundation and practical implementation of the inscribed dual band circular fractal antenna. The design methodology, simulation results, and performance analysis are presented to demonstrate the viability and advantages of using fractal geometry in Wi-Fi antenna applications. The application of the Descartes Circle Theorem in this context not only showcases the innovative approach to antenna design but also highlights the potential for further advancements in wireless communication technologies through the use of mathematical principles.

2 | Related Works

Fractal antennas have gained significant attention in recent years due to their compact size, wideband characteristics, and improved performance in wireless communication systems. This literature review examines various studies on the application of fractal antennas in Wi-Fi systems, focusing on their design, performance, and miniaturization techniques. Nejdi et al. [1] proposed a new design of a compact fractal antenna optimized for WiMAX and WLAN applications. The antenna features a rectangular radiator with integrated slots and a partial ground plane, achieving a peak gain of 6.8 dB and radiation efficiency between 91% and 94%. It operates in the frequency range of 3.2–7.5 GHz, making it suitable for various wireless communication applications, including Wi-Fi. Wank, Lu, and Chang [2] explores the miniaturization of Koch-type fractal antennas for Wi-Fi applications. By modifying the geometry of the antenna's arms, the researchers were able to develop antennas with different scales and geometries while maintaining the same base frequency. This approach allows for the creation of compact antennas with enhanced performance, suitable for space-constrained applications. A fractal ultra-wideband (UWB) antenna with circular geometry and band rejection capability utilizing the Descartes Circle Theorem [3]. This research introduces a circular fractal ultra-wideband (UWB) antenna constructed through the application of the Descartes Circle Theorem. The antenna exhibits broad frequency coverage extending beyond the Wi-Fi spectrum, and it incorporates a mechanism for rejecting undesired frequency bands. This highlights the adaptability and versatility of the proposed approach.

Fractal slot antenna with irregular circular geometry for dual wideband applications [4]. This study introduces a fractal monopole antenna fed by CPW, featuring irregular circular shapes derived from the Descartes Circle Theorem. The antenna demonstrates dual wideband properties, effectively covering the 2.4 and 5.2 GHz Wi-Fi bands while maintaining stable radiation patterns.

Fractal antenna with altered half-circle geometry utilizing the Descartes Circle Theorem for WLAN applications at 2.4/5.2 GHz [5]. This article introduces a circular fractal antenna created through the utilization of the modified half-circle shape derived from the Descartes Circle Theorem. The design accomplishes dual-band operation with commendable impedance matching and stable radiation patterns in both the 2.4 and 5.2 GHz frequency bands. On a different front, Joseph, Kumar, and Afullo [6] presented four configurations of UWB planar monopole antennas utilizing a dual-frequency square monopole patch. In the initial configuration, two rectangular patches were connected by a shorting pin, while in the second configuration, the upper patch was replaced by a wire monopole. The remaining two configurations involved connecting the first antenna configurations orthogonally, leading to a lower resonance shift towards lower frequency as the antenna size increased [7].

Several studies have focused on developing wideband and multi-band fractal antennas for Wi-Fi applications. For instance, Panday and Behera [8] designed a dual-band modified circular slot antenna for WLAN and WiMAX applications, demonstrating the versatility of fractal designs in achieving multi-frequency operation. In Pandav et al. [9] broadened the bandwidth of a square monopole antenna fed by a coaxial probe by introducing rectangular notches at the lower two corners of the patch. Patel et al. [10] suggested a method for augmenting the bandwidth of a square monopole antenna by shifting the feeding position away from the center of the patch. This asymmetrical feeding not only reduced the E-plane null but also resulted in slight offsets in the H-plane patterns.

Similarly, Patel et al. [11–14] proposed an octagonal fractal antenna with multiband and wideband capabilities, suitable for various telecommunication applications including Wi-Fi. Various strategies have been employed to enhance the performance of fractal antennas in Wi-Fi systems. These include: *Use of advanced materials*: High-performance substrates and conductive materials have been utilized to improve gain and efficiency. *Geometric modifications*: Adjustments to the fractal geometry, such as integrating slots and varying the fractal iterations, have been shown to enhance bandwidth and radiation properties. *Hybrid designs*: Combining fractal structures with other antenna types, such as patch or monopole antennas, has resulted in improved performance and functionality for Wi-Fi applications.

3 | Fractal Antenna Design

3.1 | Design Equation of Fractal Patch, Substrate and Ground

The thickness of the substrate depends on the resonant frequency of an antenna that determines the gain of an antenna. The thickness of the substrate is chosen within the range of $0.003\lambda_0 < h < 0.05\lambda_0$ [15].

$$\lambda_0 = c/f_r \tag{1}$$

where, c is the velocity of light $= 3\times10^8$ m/s. f_r is the resonant frequency.

For the frequency of 2.4 GHz, the thickness of substrate be 1.6 mm. The relative permittivity is a parameter which varies depends on the substrate material used. The material used is depends on application of antenna. The relative dielectric constant, $\in_r = 4.4$ for FR4 material has been chosen.

The theoretical formula for calculating radius of the circular patch antenna, "a" is given by

$$a = \frac{F}{\left\{1 + \frac{2h}{\pi\epsilon_r F}\left[\ln\left(\frac{\pi F}{2h}\right) + 1.7726\right]\right\}^{1/2}} \tag{2}$$

$$F = \frac{8.791\times10^9}{f_r\sqrt{\epsilon_r}} \tag{3}$$

where, h is the height of the substrate, F is fractal constant.

The effective dielectric constant of substrate is computed by using equation as

$$\in_{eff} = \frac{\in_r + 1}{2} + \frac{\in_r - 1}{2}\left[1 + 12\frac{h}{a}\right]^{-\left(\frac{1}{2}\right)} \tag{4}$$

The length (L_{sub}) and width (W_{sub}) of the substrate is calculated using the expression

$$\begin{aligned} L_{sub} &= 6h + 2a \\ W_{sub} &= 6h + 2a \end{aligned} \tag{5}$$

where, a is the radius of the circular patch.

By ensuring the substrate is sufficiently larger than the patch, you provide adequate space for the fields to decay and reduce the effects of edge radiation, leading to better performance of the antenna [16].

Steps for designing different iterations of proposed antenna is based on Descartes Circle Theorem.

The Descartes Circle Theorem asserts that when four circles are tangent to each other in the plane, with non-overlapping interiors, their curvatures follow a specific relationship, $b_j = 1/a_j$ satisfy the relation

$$\left(b_j + b_{j+1} + b_{j+2} + b_{j+3}\right)^2 = 2\left(b_j^2 + b_{j+1}^2 + b_{j+2}^2 + b_{j+3}^2\right) \tag{6}$$

where, a_j is a radius and j are the number of iterations.

Figure 1 shows the flowchart of designing and analyzing the circular fractal antenna, and the designing is as follows:

Figure 1 outlines the steps involved in designing the circular fractal antenna based on Descartes Circle Theorem:

i. *Choosing the desired operating frequencies as 2.4 and 5.55 GHz* and FR4 as dielectric material with dielectric constant $\in_r = 4.4$. For designing the proposed fractal geometry, the following procedural steps has to be followed [17].

ii. *Choosing fractal geometry*: Selects the circular fractal shape using methods such as the Descartes Circle Theorem.

iii. *Parameterizing the fractal design*: Defines key parameters:
   - Iteration-3.
   - *Scaling factor*:
     - *First iteration*: Scaling factor—85% of zeroth iteration.
     - *Second iteration*: Scaling factor—65% of first iteration.
     - *Third iteration*: Scaling factor—55% of second iteration.
     - *Feed position*: Microstrip Feeding position nurturing the antenna dimension.

iv. *Modeling and simulation*: Air Radiation boundary has been defined, lumped port excitation [18] has been denied, Frequency Sweep of 1–10 GHz has been assigned.

v. *Parametric optimization*: Iterating the design parameters guided by simulation results to achieve the desired antenna performance characteristics such as S-parameter analysis (S_{11}), VSWR, efficiency, radiation characteristic analysis, and efficiency [19].

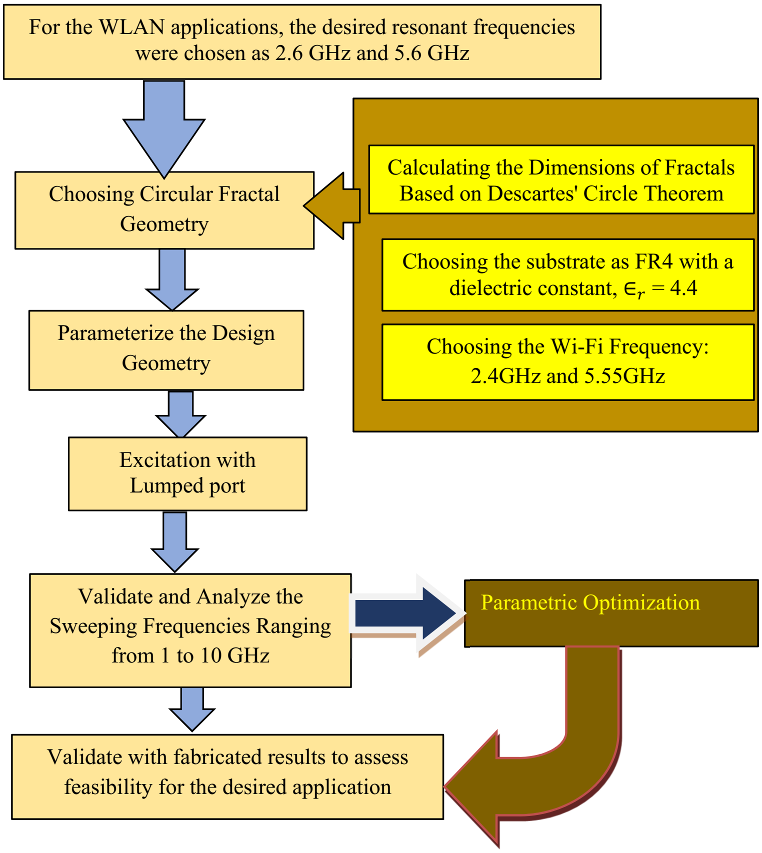

FIGURE 1 | Flowchart for designing proposed fractal antenna.

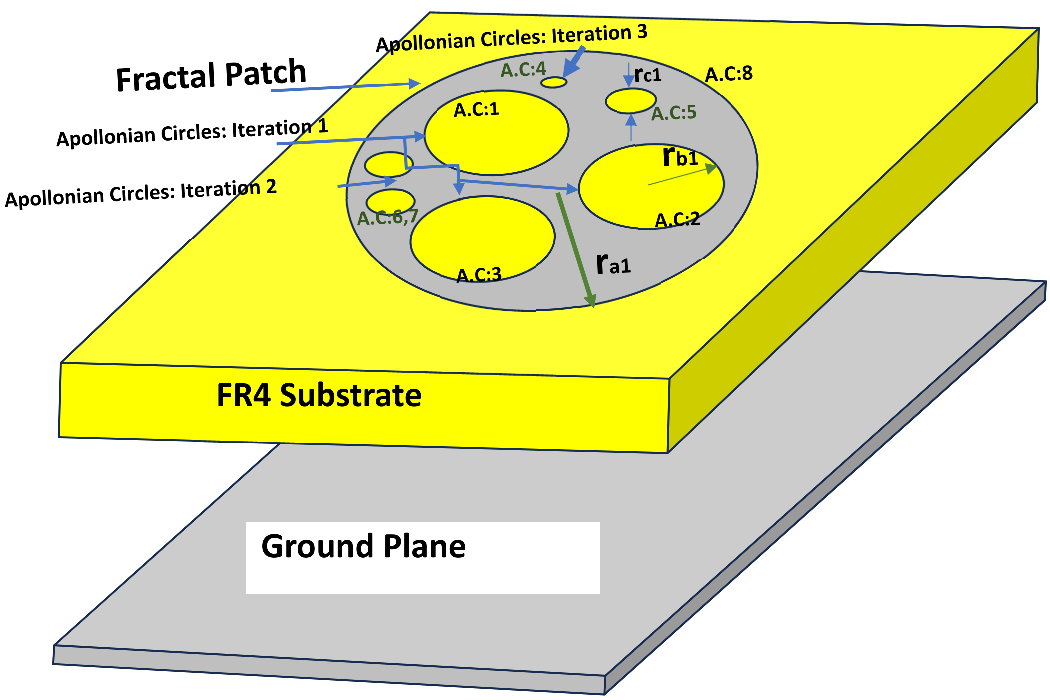

FIGURE 2 | Initial iteration of the proposed fractal antenna.

vi. *Validate with measurements*: Validating the design, boundary analysis, finite element method (FEM) analysis to carry out the simulation setup.

vii. *Performance verification*: Verifying the fabricated antennas' measurement results validating with simulated results.

TABLE 1 | Radial dimensions and curvature of Apollonian circles proposed using DC theorem.

Apollonian circle (AC)	Radius (mm)	Curvature
1	4.32	231.48
2	5.236	190.98
3	5	200
4	0.7335	1339.32
5	1.3	769.2
6	2.82	231.17
7	2	496
8	8.8	50.46

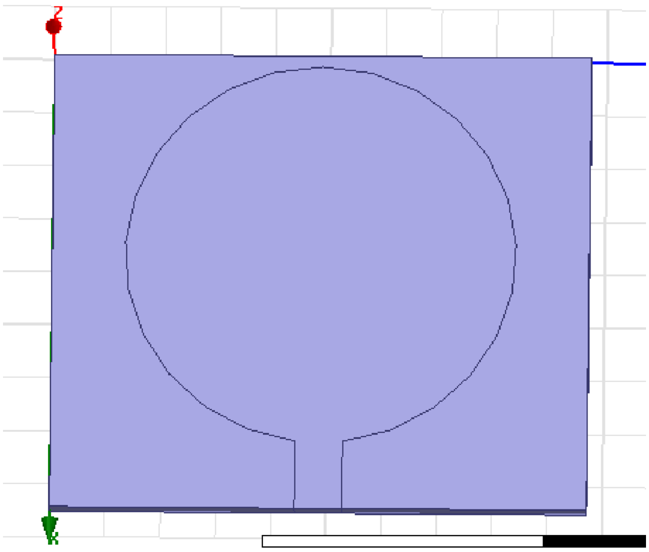

FIGURE 3 | Circular patch antenna design geometry.

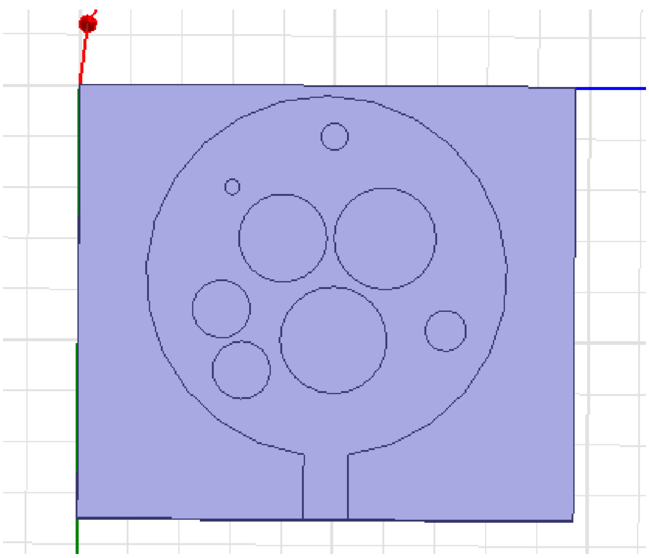

FIGURE 4 | Fabricated circular patch antenna (top view).

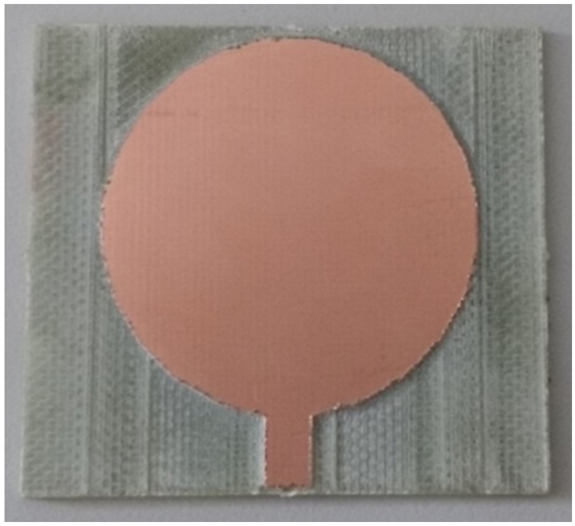

FIGURE 5 | Circular fractal antenna design geometry.

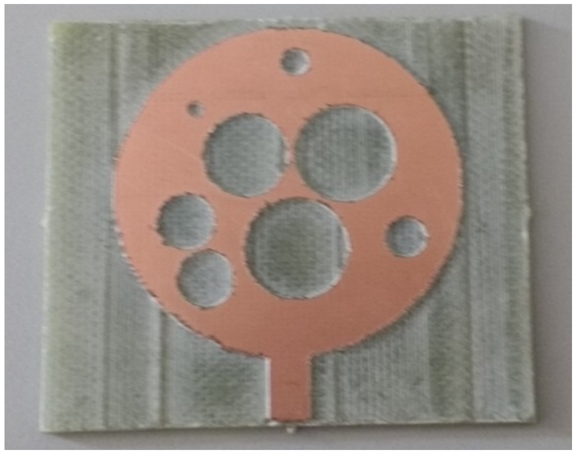

FIGURE 6 | Fabricated circular fractal antenna (top view).

3.2 | Complex Descartes Circle Theorem

In a Descartes configuration involving four circles mutually tangent to each other, their curvatures adhere to the relationship specified in [11].

$$\left(\sum_{i=1}^{4} b_i\right)^2 = 2\left(\sum_{i=1}^{4} b_i^2\right) \tag{7}$$

$$b_i = \frac{1}{a_i} \tag{8}$$

Any arrangement of four circles that are mutually tangent, following Descartes' configuration, with curvatures represented by a_j and centers denoted as $z_j = x_j + i * y_j$, meets the specified conditions [11].

$$\left(\sum_{i=1}^{4} b_i z_j\right)^2 = 2\left(\sum_{i=1}^{4} b_i z_j\right) \tag{9}$$

$$Z_j = x_j + y_j \tag{10}$$

where, Z_j is circle center position represented in complex form.

The radii of the three identical inner circles are determined using Equation (11). The Figure 2 shows the placement and size of these initial circles which form the basis for further iterations. The curvature, assuming a normal pointing outward ($a=-1$), is determined on the premise that the original circular aperture represents a unit circle [20].

During the self-similar design iteration with $i=1$, the radii of the three identical inner circles [21], are determined through the application of equation [11] and showcased as.

$$r_{d1} = r_{c1} = r_{b1} = 6/(6+4\sqrt{3}) \tag{11}$$

Utilizing the Descartes Circle Theorem, curvatures for the initial four circles are calculated, and Table 1 is generated to encompass approximately five iterations.

During the second phase, the radii of five circles [22] are determined based on the initial four circles established in the first stage.

$$f_j^i = a_j + b_j + c_j + 2\sqrt{a_j b_j + b_j c_j + a_j c_j} \tag{12}$$

where, f_j^i is the radius of second iterative circles.

Where circle 1, 2, and 3 were parent circles. Using the parent circles as base, the 4th circle's radius and position were computed using Descartes Equation. For 2nd iteration, 5th circle's radius and position were computed using the base circles 2, 3, and 4. These steps were repeated by changing the base circle. The iteration process has been repeated till obtaining the desired results.

4 | Parametric Analysis of Circular Patch and Fractal Antenna

The paper discusses various performance metrics, including but not limited to bandwidth, reflection coefficient (S_{11}), and directivity. These metrics are crucial for evaluating the efficiency of the proposed antenna design in practical Wi-Fi scenarios. Rigorous simulations and modeling are conducted to validate the proposed design. Advanced tools and techniques [23, 24] are employed to analyze the antenna's behavior and performance under different conditions. Figures 3 and 4 show the top view of simple circular patch antenna and fabricated circular patch antenna respectively which is designed for the resonant frequency of 2.4 and 5.5 GHz. The feeding techniques used in the antenna is line feed and the excitation used is wave port excitation. The circular patch and the line fed were united. The ground plane and the patch were made of copper material. The boundary is considered to be an air medium. Figures 5 and 6 present the top view of the proposed circular fractal antenna [25] and fabricated circular fractal antenna designed for 2.4 and 5.55 GHz frequencies. The antenna uses wave port excitation and line feeding techniques, with FR4 as the substrate material (dielectric constant of 4.4). The ground plane and patch are made of copper, with an air medium boundary.

4.1 | Circular Patch-S-Parameter (S_{11}) Analysis

The article presents a comprehensive simulation results and compares them against the desired specifications. The discussion interprets these findings, highlighting the effectiveness of the dual-band circular fractal antenna for Wi-Fi applications. Figure 7 shows the reflection coefficient (S_{11}) of the circular patch antenna. Ideally, the S-parameter (S_{11}) should be less than −10 dB [26]. At 2.4 and 5.55 GHz, the simulated S-parameters (S_{11}) are −18.1 and −13.51 dB, respectively. The measured results, however, show S-parameters (S_{11}) of −17.9 dB at 2.4 GHz and −13.0 dB at 5.55 GHz, with a −10 dB bandwidth of 21%. The bandwidth was calculated using the appropriate equation, indicating that the circular patch antenna has relatively low gain.

$$\text{Bandwidth} = \frac{f_2 - f_1}{f_r}$$

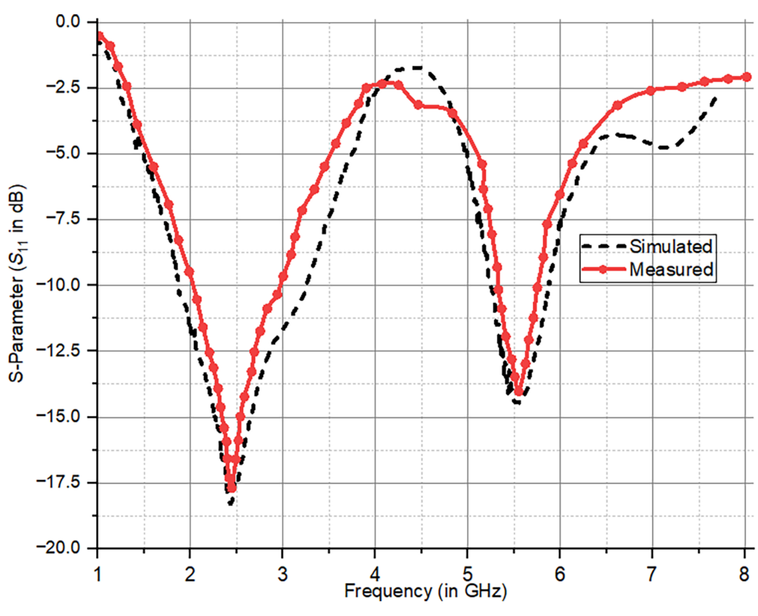

FIGURE 7 | S-parameter (S_{11}) analysis for circular patch antenna.

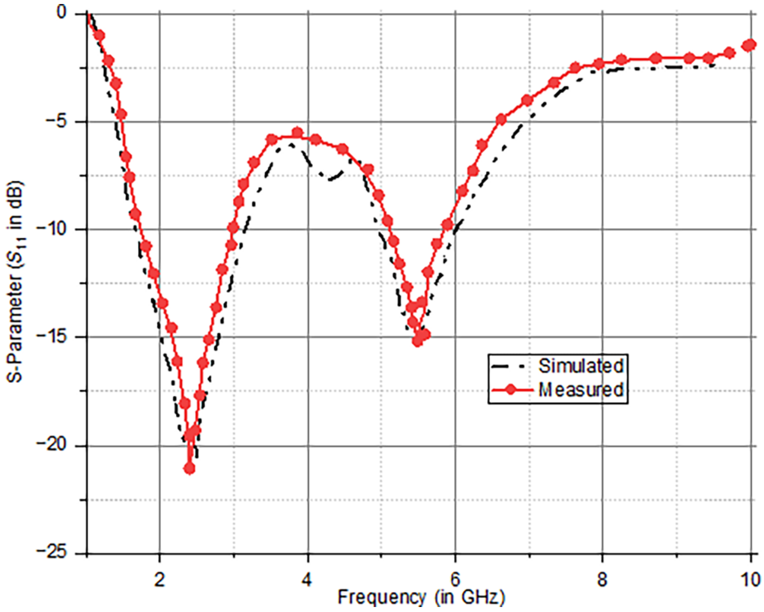

FIGURE 8 | S-parameter (S_{11}) analysis for circular fractal antenna.

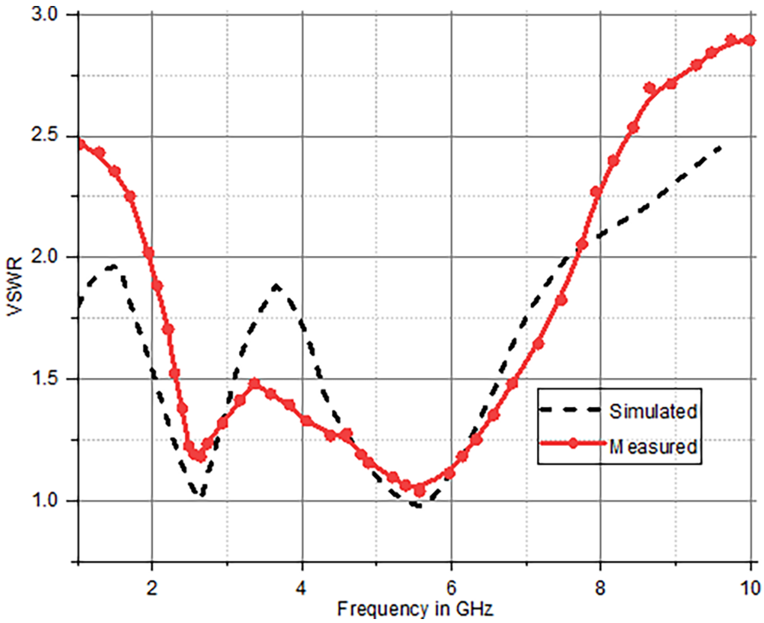

FIGURE 9 | VSWR of circular patch antenna for impedance matching analysis.

where, f_r = resonant frequency, f_1 = minimum frequency, f_2 = maximum frequency.

4.2 | Circular Fractal Patch-*S*-Parameter (S_{11}) Analysis

Figure 8 shows the S-parameter (S_{11}) analysis for the circular fractal antenna. The simulation results indicate a return loss of −21.0 dB at 2.4 GHz and −15.0 dB at the second frequency of 5.55 GHz. In comparison, the measured results show S-parameter (S_{11}) values of −22.0 dB at 2.4 GHz and −15.5 dB at 5.55 GHz, with a −10 dB bandwidth of 31.7%. These results demonstrate that the antenna operates at multiple frequencies, making it suitable for Wi-Fi applications. Additionally, the S-parameter (S_{11}) is also significant at other frequencies, which are considered harmonic frequencies.

4.3 | Circular Patch-VSWR Analysis

Figure 9 shows the VSWR (Voltage Standing Wave Ratio) for the circular patch antenna. Ideally, the VSWR should be as close to 1 as possible for the best case, with higher values indicating poorer performance. Practically, a VSWR of up to 2 is considered acceptable. At 2.4 and 5.55 GHz, the simulated VSWR values are 1.1 and 0.9, respectively, while the measured results show VSWR values of 1.2 and 1.15 for 2.4 and 5.55 GHz, respectively. These results

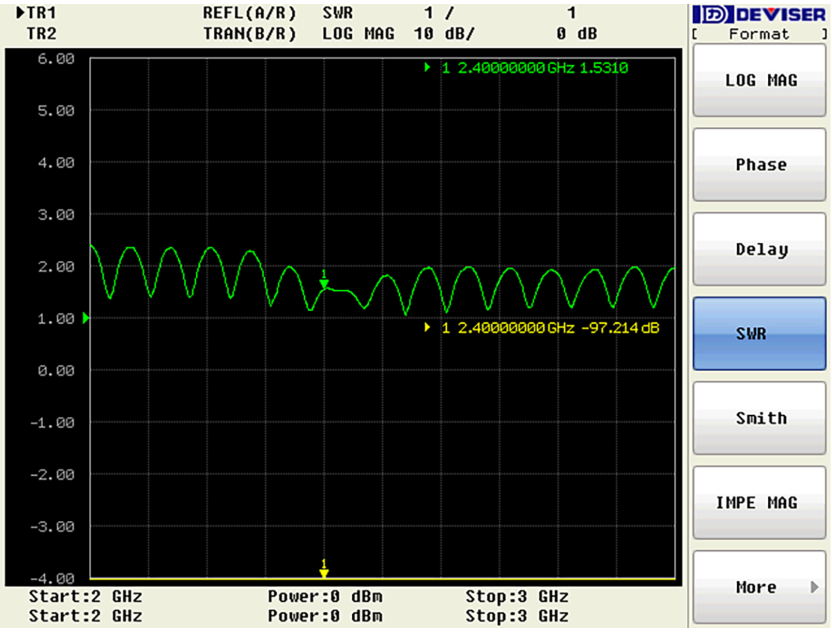

FIGURE 10 | VSWR analysis for circular patch antenna (screenshot from VNA).

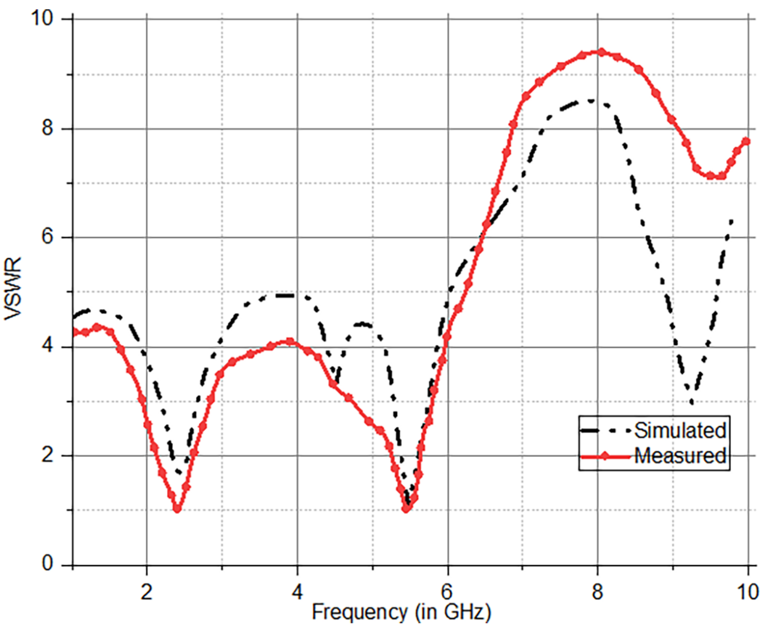

FIGURE 11 | VSWR analysis of circular fractal antenna for impedance matching analysis.

suggest that the antenna does not perform effectively at 2.4 and 5.55 GHz, indicating it may not be suitable for Wi-Fi applications. Figure 10 shows the graphical representation (screenshot) of VSWR analysis for circular patch antenna.

4.4 | Circular Fractal Patch-VSWR Analysis

Figure 11 shows the VSWR of the circular fractal antenna. At 2.4 and 5.55 GHz, the simulated VSWR is 1.7 and 1.0, compared to the measured VSWR of 1.1 and 1.0, respectively. Compared to the circular patch, the circular fractal antenna has a lower VSWR, indicating better impedance matching. Hence, the reflected signal at the input port is minimized, resulting in maximum gain. Figure 12 shows the graphical representation (screenshot) of VSWR analysis for circular fractal antenna.

4.5 | Output Impedance Analysis

Fractal antennas often exhibit multiband behavior due to their self-similar structure. The resonant frequencies $f_{r,n}$ for different bands can be approximated by scaling laws based on the fractal iteration:

$$f_{r,n} = f_{r,n0} \cdot S^n \tag{13}$$

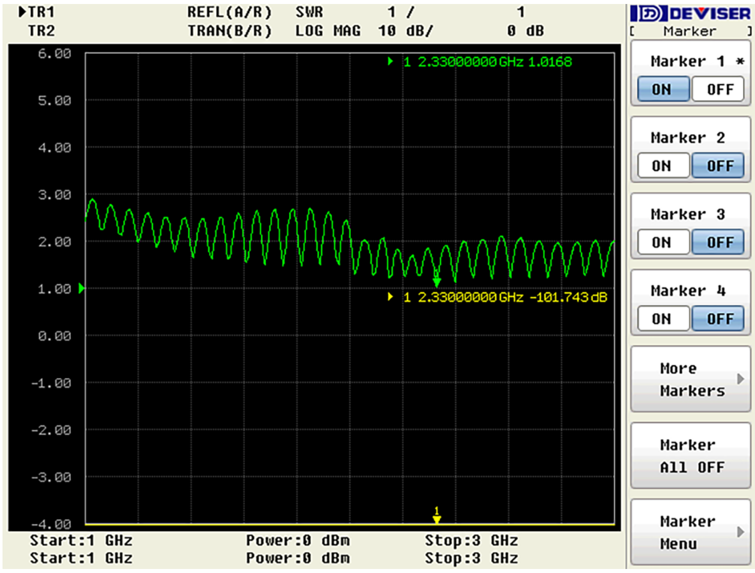

FIGURE 12 | VSWR analysis for circular fractal antenna (screenshot from VNA).

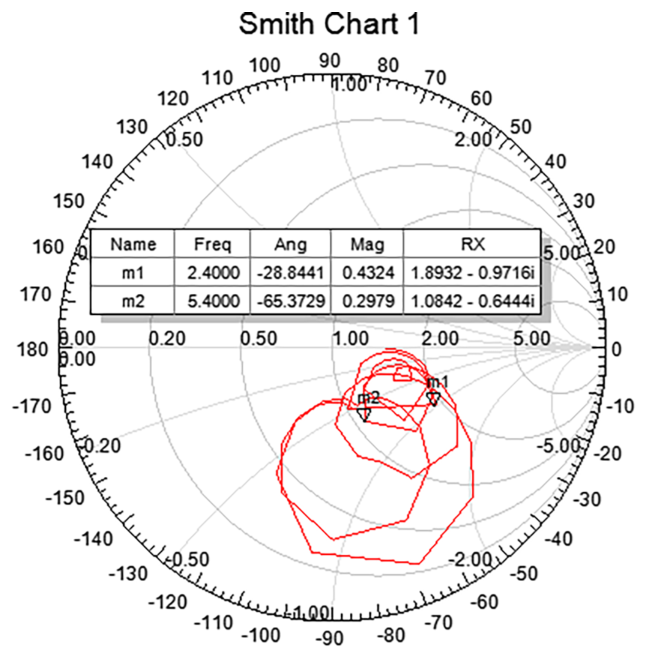

FIGURE 13 | Output impedance of circular patch antenna (simulated).

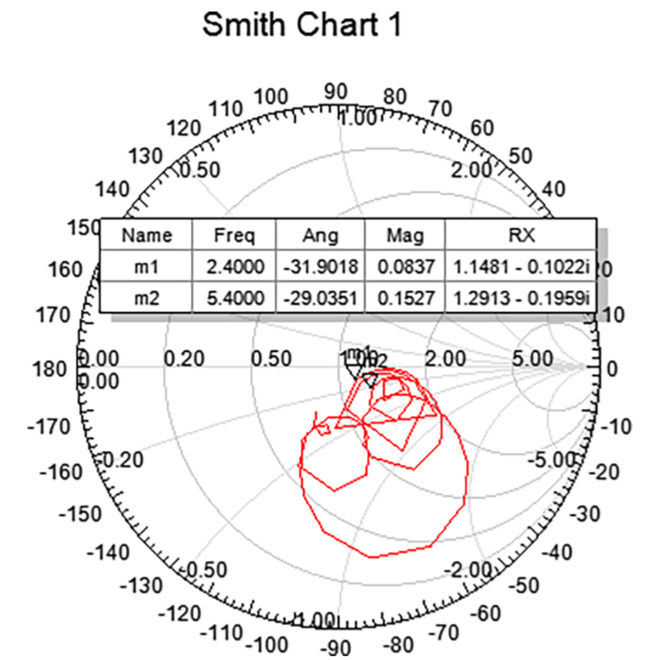

FIGURE 14 | Output impedance of circular fractal antenna (simulated).

where, $f_{r,0}$ is the fundamental resonant frequency and S is the scaling factor.

Figure 13 shows the output impedance of the circular patch antenna. Ideally, the antenna output impedance should be $1 + 1j$ or 50 Ω. At 2.4 and 5.55 GHz the antenna impedance is $1.8932 - 0.9716j$ and $1.0842 - 0.6644j$, respectively. It seems that the reactance part of the impedance is capacitive.

The Figure 14 shows the output impedance of the circular fractal antenna. At 2.4 and 5.5 GHz the impedance of the antenna is $1.1481 - 0.1022j$ and $1.2913 - 0.1959j$, respectively. By comparing the circular patch and circular fractal antennas, the fractal antenna has an impedance closer to unity. Hence, the fractal antenna has a self-impedance matching property. Figures 15 and 16 show the output impedance analysis of proposed circular fractal antenna (VNA screenshot). The output impedance of fractal antenna is 56 Ω and 129 pH inductor at 2.4 GHz. By comparing fractal and simple patch, fractal has good impedance matching, less VSWR and high reflection coefficient (S_{11}). From the fabricated results, fractal antennas are good and enough for practical application.

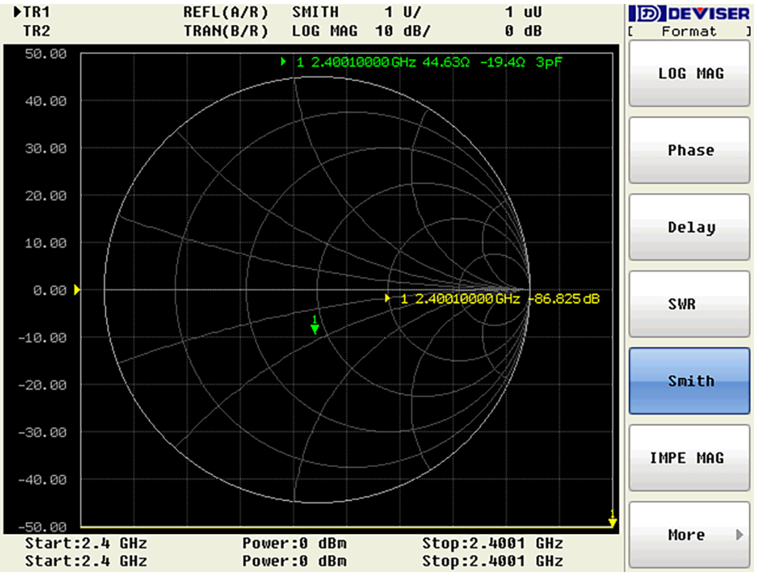

FIGURE 15 | Output impedance of circular patch antenna (VNA screenshot).

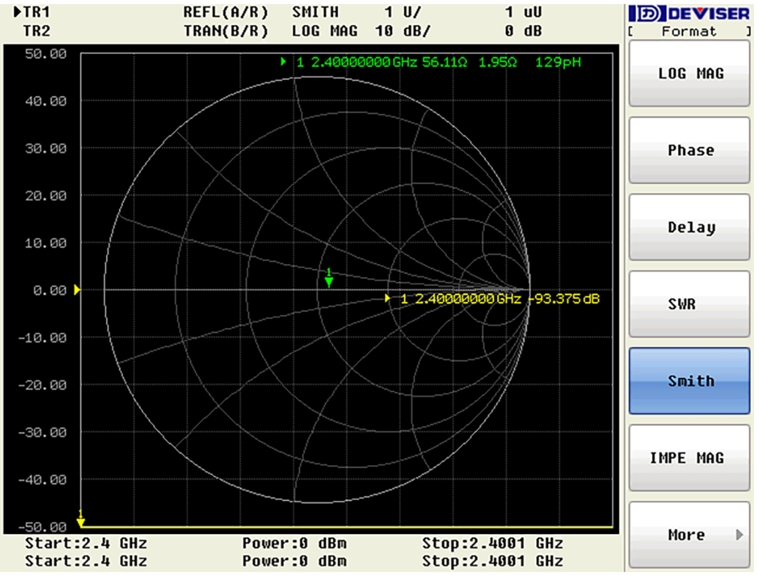

FIGURE 16 | Output impedance of circular fractal antenna (VNA screenshot).

4.6 | Circular Fractal Patch—Radiation Pattern Analysis

Figure 17 shows the radiation pattern of the circular fractal antenna. It depicts that the antenna radiates in a unidirectional pattern, with some radiation at the back, known as side lobes. The front-to-back ratio for the circular patch antenna is 101.4. The central axis in the radiation pattern is known as the beam axis. At 0° on the beam axis, the gain is 11.7920. Compared to the circular patch antenna, the circular fractal antenna has a higher gain and front-to-back ratio. The HPBW (Half Power Beam Width) of the antenna is 100°, and the directivity of the antenna is also higher than that of the circular patch.

The pattern is more similar to the simulated antenna results. The front to back ratio of the antenna is 119.04. The antenna measured the pattern for every 0.5° angle with respect to isotropic antenna. The isotropic antenna used for the gain measurement have gain of 60 dBi and the gain of AUT obtained is −42 dB. The gain of the antenna is measured by using below formula,

$$\text{Gain(dBi)} = \text{Gain of isotropic antenna} + \text{Gain of AUT}$$
$$= 60\ \text{dBi} + (-42\ \text{dB}) = 18\ \text{dB}$$

The designed DC theorem based circular patch fractal antenna earned better results, as shown the comparison Table 2.

Based on the observations, it is evident that all designs resulted in dual-band and wideband characteristics. Notably, employing a cut as an additional measure to achieve wideband functionality proved to be an effective solution. This improvement is reflected in the bandwidth efficiency, which increased from 21% at the

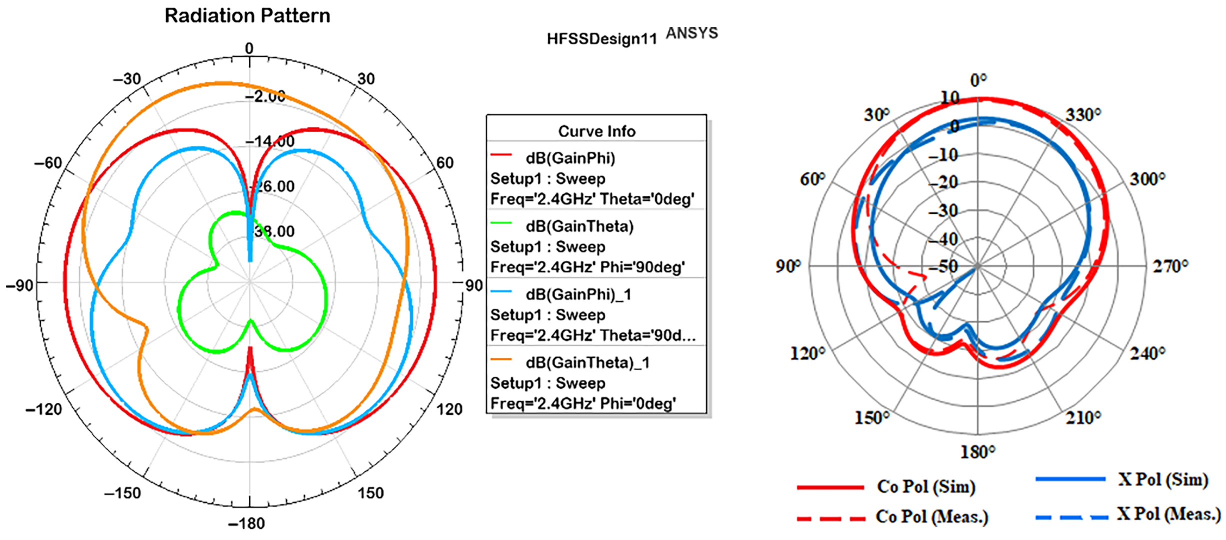

(a) **2.4 GHz** **(b)** **5.55 GHz**

FIGURE 17 | 2D far field radiation pattern at 2.4 and 5.55 GHz of proposed fractal antenna.

TABLE 2 | Parametric analysis of characteristic parameters of conventional circular patch antenna with proposed circular fractal antenna.

	Circular patch antenna				Proposed circular fractal antenna			
	Simulated		Measured		Simulated		Measured	
Parameters	$f_r = 2.4$ GHz	$f_r = 5.55$ GHz	$f_r = 2.4$ GHz	$f_r = 5.55$ GHz	$f_r = 2.4$ GHz	$f_r = 5.55$ GHz	$f_r = 2.4$ GHz	$f_r = 5.55$ GHz
S-parameter (S_{11}) (dB)	−18.1	−13.51	−17.9	−13.0	−21.0	−15.0	−22	−15.5
VSWR	1.1	0.9	1.2	1.15	1.7	1.0	1.1	1.0
Impedance (Ω)	$1.8 - 0.97j$	$1.08 - 0.6j$	$4.4 + 1.2j$	$1.3 - 2.1j$	$1.1 - 0.1j$	$1.2 - 0.19j$	$1.89 + 4.99j$	$5.09 + 3.64j$
Peak gain (dBi)	3.4	3.6	3.3	3.2	10.2	9.4	11.792	9.4
Front to back ratio	94.75	92.3	101.4	119.04	96.2	99.3	97.2	96.4
Bandwidth improvement %	21	43	27	38	24.5	38.2	28.2	36.4
Efficiency improvement	—	—	—	—	35%	55.9%	29%	48%

third stage to 35% for the circular patch design and further to 55.9% for the circular fractal at the first frequency. However, it is worth noting that in both cases, the disparities between gain and directivity were not substantial.

Table 3 shows the comparative analysis of proposed circular fractal antenna with existing relevant antennas shows the exceptional characteristics in terms of gain, bandwidth, and efficiency.

5 | Summary of the Research Work

The key findings of proposed antenna:

i. *Design and theoretical framework*:
- The manuscript focuses on modeling a dual-band circular fractal antenna using the Descartes Circle Theorem for Wi-Fi applications.
- The fractal antenna geometry, characterized by self-similar patterns, enhances performance in the 2.4 and 5.2 GHz bands.
- The Descartes Circle Theorem helps overcome issues related to the Apollonian circle, improving antenna gain and miniaturization.

ii. *Performance metrics*:
- *Reflection coefficient* (S_{11}): The circular fractal antenna exhibits a significant improvement in the reflection coefficient (S_{11}) at the resonant frequencies of 2.4 and 5.55 GHz, achieving −22 and −15.5 dB, respectively, compared to −17.9 and −13 dB in a conventional circular patch antenna.
- *Gain*: The fractal antenna shows a gain of 11.7920 dB, substantially higher than the 3.3 dBi gain of the conventional patch antenna.

TABLE 3 | Parametric analysis of proposed circular fractal antenna with existing relevant antennas.

References	Novelty	$L \times W$ (mm)	Resonating frequencies (GHz)	Peak gain (dBi)	Bandwidth improvement %	Maximum efficiency improvement in %
[2]	Hexagonal fractal patch	75 × 75	1.575 and 5.9	3.2	23.7	35
[8]	Triangular patch, slot	30 × 28	2.8 and 5.7	4.1	19.94	44
[9]	Cresent shape patch	31 × 35	11.30 and 18.07	3.8	35.4	32
[11]	Fractal, L shape slot and SRR	30 × 24.8	3.3 and 5.5	2.6	29.6	28
[12]	U slot	30 × 40	1.8 and 2.4	5.3	36.4	37.6
[13]	SRR	22 × 24	2.48 and 3.49	4.38	21.4	48.1
[27]	Quarter-mode substrate integrated waveguide, Fractal, CSRR	23 × 20.5	Between 4.96 and 5.88 (tunable by rotating the CSRR)	6.2	18.7	42.8
[28]	Slot, ELC, Koch Fractal	40 × 40	1.5, 5.4	5.1	27.4	24.9
Proposed circular fractal	Descartes Circle Theorem based apollonian circular patch	27.84 × 23.25	2.4 and 5.55	11.79 and 9.4	38.2	55.9

- *Radiation pattern*: The antenna radiates in a unidirectional pattern with a high front-to-back ratio of 101.4, indicating better directionality compared to the conventional design.

iii. *Design and fabrication*:
- The antenna design incorporates circular fractal patterns, utilizing self-similarity for enhanced performance.
- The antenna was fabricated through a photo-etching process and tested, validating the theoretical and simulation results.

iv. *Advantages of fractal design*:
- Fractal antennas offer increased bandwidth, multi-band operation, reduced size, and optimal smart antenna technology.
- The fractal design results in "fractal loading," allowing for significant size reduction while maintaining performance.
- The designed antenna operates effectively at both target frequencies, demonstrating broad bandwidth efficiency and stable radiation patterns.

v. *Validation and practical applications*:
- The prototype was tested using network analyzers and antenna chambers, confirming the simulation outcomes.
- The antenna's dual-band functionality makes it suitable for various Wi-Fi applications, including future wireless technologies.

5.1 | Significance

- *Enhanced performance*: The improved reflection coefficient and gain indicate a more efficient antenna design, crucial for reliable Wi-Fi communication.
- *Miniaturization*: The ability to achieve compact antenna designs without compromising performance is significant for modern wireless communication devices.
- *Broadband and multi-band operation*: The fractal design's ability to operate over multiple bands and exhibit ultra-wideband functionality is vital for accommodating emerging wireless technologies.
- *Practical utility*: The successful integration with RF circuits and systems enhances the antenna's applicability in real-world scenarios, making it a valuable contribution to wireless communication advancements.
- These findings underscore the potential of fractal antennas in achieving high performance and compactness, crucial for the evolving demands of wireless communication systems.

6 | Conclusion

The article exposed the significance of the proposed design in the context of Wi-Fi and wireless communication systems. The application of the Descartes Circle Theorem has proven valuable in the creation of dual-band circular fractal antennas tailored for Wi-Fi applications. The studies examined underscore the efficacy of this method in achieving target operating frequencies, bandwidths, and radiation characteristics. Future research is focused on expanding the capabilities of these antennas to include wider bandwidths, multi-band operation, and seamless integration with real-world systems. A circular patch antenna was simulated for frequencies of 2.4 and 5.55 GHz using HFSS 13.0. It achieved a reflection coefficient (S_{11}) of −18.1 and −13.51 dB at 2.4 and 5.55 GHz, respectively, with a peak gain of 3.6 dBi. To improve the gain and reflection coefficient (S_{11}), achieve a low profile, and enable self-impedance matching, a circular fractal antenna was designed using the Descartes Circle Theorem. The simulated results showed a reflection coefficient (S_{11}) of −21.0

and −15.0 dB at 2.4 and 5.55 GHz, respectively, with a gain of 11.79 dBi. The antennas were fabricated using a PCB prototype machine and tested using a VNA. The fabricated circular fractal antenna had reflection coefficients (S_{11}) of −22 and −15.5 dB at 2.4 and 5.55 GHz, respectively. The analysis indicates that the circular fractal antenna has higher gain and better reflection coefficients (S_{11}) than the circular patch antenna. The future scope of the project includes eliminating harmonic frequencies using a band-stop filter. The report introduces compact, multi-band circular fractal designs as a noteworthy alternative to conventional antenna systems in mobile wireless receivers. Despite various research efforts by scholars in electrical engineering, fractal antenna technology remains in its early stages, with limited existing literature. The study's findings suggest promising research opportunities in antenna configuration. Consequently, the researcher proposes that future investigations explore integrating reusable technology to enhance the adaptability of antennas, enabling seamless switching to the desired operating range.In the future, authors may explore emerging technologies [29–34] and their impact on wireless communication systems [29–34].

Author Contributions

SatheeshKumar Palanisamy: conceptualization, investigation, validation, software, data curation. **Anitha R. Vaddinuri:** investigation, validation, formal analysis, project administration, software. **Arfat Ahmad Khan:** conceptualization, methodology, writing – review and editing, validation. **Muhammad Faheem:** conceptualization, data curation, supervision, resources, validation, visualization, writing – review and editing.

Conflicts of Interest

The authors declare no conflicts of interest.

Data Availability Statement

Data sharing not applicable to this article as no datasets were generated or analysed during the current study.

References

1. I. H. Nejdi, S. Bri, M. Marzouk, et al., "UWB Circular Fractal Antenna With High Gain for Telecommunication Applications," *Sensors* 23 (2023): 4172, https://doi.org/10.3390/s23084172.

2. E. Wang, X. Liu, and H. Chang, "Wideband Circular Polarized Fractal Antenna for RFID/WiMAX/WLAN Applications," *Progress in Electromagnetics Research Letters* 111 (2023): 111–120.

3. O. Benkhadda, M. Saih, S. Ahmad, et al., "A Miniaturized Tri-Wideband Sierpinski Hexagonal-Shaped Fractal Antenna for Wireless Communication Applications," *Fractal and Fractional* 7, no. 2 (2023): 115.

4. M. Kaur, R. Krishan, J. S. Sivia, and N. Kaur, "Shuffled Frog Leaping Algorithm Based Circular Patterns Loaded Ring Shaped Fractal Antenna for Multistandard Wireless Applications," *AEU-International Journal of Electronics and Communications* 176 (2024): 155123.

5. R. H. Elabd and A. J. A. Al-Gburi, "Design and Optimization of a Circular Ring-Shaped UWB Fractal Antenna for Wireless Multi-Band Applications Using Particle Swarm Optimization," *Progress in Electromagnetics Research B* 106 (2024): 101–112.

6. E. Joseph, P. Kumar, and T. Afullo, "Design and Performance Evaluation of a Second-Order Iterated Circular Minkowski Fractal Antenna for Ultra-Wideband Applications," *Fractal and Fractional* 7, no. 11 (2023): 806.

7. Y. Anand and V. Nath, "Dual Polarized Gain Enrichment of a Low-Cost Multi-Band Circular Fractal Antenna Using Tunable Stacked FSS for Wireless Applications," *Iranian Journal of Science and Technology, Transactions of Electrical Engineering* 48 (2024): 1373–1391.

8. S. Pandav and S. K. Behera, "Circularly Polarized 2 × 2 Fractal Antenna Array for Space Borne Tracking Applications," *AEU-International Journal of Electronics and Communications* 178 (2024): 155249.

9. S. Pandav, G. Sadhukhan, T. K. Das, S. K. Behera, and M. Mohanty, "π-Shaped Circularly Polarized High-Gain Minkowski Fractal Antenna for Radar Applications," *International Journal of Communication Systems* 37, no. 2 (2024): e5648.

10. U. Patel, T. Upadhyaya, V. Sorathiya, et al., "Split Ring Resonator Geometry Inspired Crossed Flower Shaped Fractal Antenna for Satellite and 5G Communication Applications," *Results in Engineering* 22 (2024): 102110, https://doi.org/10.1016/j.rineng.2024.102110.

11. U. Patel, T. Upadhyaya, A. Desai, R. Pandey, and K. Pandya, "Dual-Band Compact Split-Ring Resonator-Shaped Fractal Antenna With Defected Ground Plane for Sub-6-GHz 5G and Global System for Mobile Communication Applications," *International Journal of Communication Systems* 35, no. 7 (2022): e5105, https://doi.org/10.1002/dac.5105.

12. U. Patel, M. Parekh, A. Desai, and T. Upadhyaya, "Wide Slot Tri-Band Antenna for Wireless Local Area Network/World-Wide Interoperability for Microwave Access Applications," *International Journal of Communication Systems* 34 (2021): e4897, https://doi.org/10.1002/dac.4897.

13. U. Patel and T. K. Upadhyaya, "Design and Analysis of Compact μ-Negative Material Loaded Wideband Electrically Compact Antenna for WLAN/WiMAX Applications," *Progress in Electromagnetics Research M* 79 (2019): 11–22, https://doi.org/10.2528/PIERM18121502.

14. U. Patel, T. Upadhyaya, A. Desai, R. Pandey, K. Pandya, and B. Kundaliya, "3 × 3 Split-Ring Resonators Array-Inspired Defected Ground Plane Antenna for 2.4/5.5 GHz Wireless LAN Applications," in *Proceedings of International Conference on Communication and Artificial Intelligence*, vol. 435, eds. V. Goyal, M. Gupta, S. Mirjalili, and A. Trivedi (Singapore: Lecture Notes in Networks and Systems, Springer, 2022), https://doi.org/10.1007/978-981-19-0976-4_1.

15. N. Sathishkumar, S. Palanisamy, R. Natarajan, et al., "Design of Dual Mode Antenna Using CMA and Broadband Dual-Polarized Antenna for 5G Networks," *Scientific Reports* 14 (2024): 15553, https://doi.org/10.1038/s41598-024-66515-x.

16. E. Suganya, T. Prabhu, S. Palanisamy, and A. O. Salau, "Design and Performance Analysis of L-Slotted MIMO Antenna With Improved Isolation Using Defected Ground Structure for S-Band Satellite Application," *International Journal of Communication Systems* 8 (2024): e5901, https://doi.org/10.1002/dac.5901.

17. N. Sathishkumar, S. Palanisamy, O. I. Khalaf, R. Natarajan, S. Algburi, and H. Hamam, "Experimental Investigation of a Dual Mode Antenna Using Characteristic Mode Analysis With Enhanced Directivity for GSM/5G Applications," *Heliyon* 10, no. 11 (2024): e32217, https://doi.org/10.1016/j.heliyon.2024.e32217.

18. V. R. Anitha, S. Palanisamy, O. I. Khalaf, S. Algburi, and H. Hamam, "Design and Analysis of SRR Based Metamaterial Loaded Circular Patch Multiband Antenna for Satellite Applications," *ICT Express* 10, no. 4 (2024): 836–844, https://doi.org/10.1016/j.icte.2024.05.002.

19. I. Jebril, P. Dhanaraj, G. M. Abdulsahib, S. K. Palanisamy, T. Prabhu, and O. I. Khalaf, "Analysis of Electrically Couple SRR EBG Structure for Sub 6 GHz Wireless Applications," in *Advances in Decision Sciences*, vol. 26 (Taiwan: Asia University, 2022), 102–123.

20. S. Palanisamy and B. Thangaraju, "Design and Analysis of Clover Leaf-Shaped Fractal Antenna Integrated With Stepped Impedance Resonator for Wireless Applications," *International Journal of Communication Systems* 35, no. 11 (2022): e5184, https://doi.org/10.1002/dac.5184.

21. N. Subramanian, S. Palanisamy, and T. Nivethitha, "Achieving Secured Medical Network (SMN) Through Stateless Mechanism and SkeyM in Medical-Internet of Things (M-IoT)," *Journal of Engineering and Applied Science* 71 (2024): 128, https://doi.org/10.1186/s44147-024-00460-4.

22. E. Suganya, T. Prabhu, S. Palanisamy, P. K. Malik, N. Bilandi, and A. Gehlot, "An Isolation Improvement for Closely Spaced MIMO Antenna Using λ/4 Distance for WLAN Applications," *International Journal of Antennas and Propagation* 2023 (2023): 4839134, https://doi.org/10.1155/2023/4839134.

23. S. Palanisamy, B. Thangaraju, O. I. Khalaf, Y. Alotaibi, S. Alghamdi, and F. Alassery, "A Novel Approach of Design and Analysis of a Hexagonal Fractal Antenna Array (HFAA) for Next-Generation Wireless Communication," *Energies* 14, no. 19 (2021): 6204, https://doi.org/10.3390/en14196204.

24. S. Palanisamy, B. Thangaraju, O. I. Khalaf, Y. Alotaibi, and S. Alghamdi, "Design and Synthesis of Multi-Mode Bandpass Filter for Wireless Applications," *Electronics* 10, no. 22 (2021): 2853, https://doi.org/10.3390/electronics10222853.

25. S. Kumar and T. Balakumaran, "Modeling and Simulation of Dual Layered U-Slot Multiband Microstrip Patch Antenna for Wireless Applications," *Nanoscale Reports* 4, no. 1 (2021): 15–18, https://doi.org/10.26524/nr.4.3.

26. G. M. Abdulsahib, D. S. Selvaraj, A. Manikandan, et al., "Reverse Polarity Optical Orthogonal Frequency Division Multiplexing for High-Speed Visible Light Communications System," *Egyptian Informatics Journal* 24, no. 4 (2023): 100407, https://doi.org/10.1016/j.eij.2023.100407.

27. K. Ganesan, S. Palanisamy, V. Krishnasamy, A. O. Salau, V. Rathinam, and S. G. Seeni Nayakkar, "Hybrid Photovoltaic/Thermal Performance Prediction Based on Machine Learning Algorithms With Hyper-Parameter Tuning," *International Journal of Sustainable Energy* 43, no. 1 (2024): 2364226, https://doi.org/10.1080/14786451.2024.2364226.

28. S. Palanisamy, S. S. Rubini, O. I. Khalaf, et al., "Multi-Objective Hybrid Split-Ring Resonator and Electromagnetic Bandgap Structure-Based Fractal Antennas Using Hybrid Metaheuristic Framework for Wireless Applications," *Scientific Reports* 14 (2024): 3288, https://doi.org/10.1038/s41598-024-53443-z.

29. M. Faheem, H. Kuusniemi, B. Eltahawy, M. S. Bhutta, and B. Raza, "A Lightweight Smart Contracts Framework for Blockchain-Based Secure Communication in Smart Grid Applications," *IET Generation Transmission and Distribution* 18 (2024): 625–638, https://doi.org/10.1049/gtd2.13103.

30. M. Faheem, B. Raza, M. S. Bhutta, and S. H. Madni, "A Blockchain-Based Resilient and Secure Framework for Events Monitoring and Control in Distributed Renewable Energy Systems," *IET Blockchain* (2024): 1–15, https://doi.org/10.1049/blc2.12081.

31. M. Burhan, H. Alam, A. Arsalan, et al., "A Comprehensive Survey on the Cooperation of Fog Computing Paradigm-Based IoT Applications: Layered Architecture, Real-Time Security Issues, and Solutions," *IEEE Access* 11 (2023): 73303–73329, https://doi.org/10.1109/ACCESS.2023.3294479.

32. M. Faheem, M. A. Al-Khasawneh, A. A. Khan, and S. H. Madni, "Cyberattack Patterns in Blockchain-Based Communication Networks for Distributed Renewable Energy Systems: A Study on Big Datasets," *Data in Brief* 53 (2024): 110212.

33. M. Faheem and M. A. Al-Khasawneh, "Multilayer Cyberattacks Identification and Classification Using Machine Learning in Internet of Blockchain (IoBC)-Based Energy Networks," *Data in Brief* 54 (2024): 110461.

34. M. A. Al-Khasawneh, M. Faheem, E. A. Aldhahri, A. Alzahrani, and A. A. Alarood, "A MapReduce Based Approach for Secure Batch Satellite Image Encryption," *IEEE Access* 11 (2023): 62865–62878.